CrossMark

Aeromagnetic data for mapping geologic contacts at Samr El-Qaa area, North Eastern Desert, Egypt

Ahmed Mohammed Eldosouky[1]

Abstract

Delineating the edges of different magnetized sources represents a fundamental tool for interpreting and mapping rock boundaries of magnetic data. The present study deals with the enhancement of reduced to the pole map (RTP) of Samr El-Qaa area, North Eastern Desert, Egypt, to map deep and surface geologic contacts. The edge detection of geologic contacts is ensured by the upward continuation of reduced to the pole data at an altitude of 3 km, followed by the calculation of theta derivative and horizontal tilt angle derivative (HTAD) for RTP and upward continuation (3 km). The results obtained from the application of these techniques showed that the theta derivative delineates RTP source edges well, but the response of deeper sources is diffused. While HTAD presented well, responds to shallow and deep sources and also the edges of the sources were delineated well. HTAD showed a much sharper gradient over the edges of the magnetized sources at Samr El-Qaa area. The interpreted structural trends derived from shallow and deep Theta and HTAD maps of Samr El-Qaa territory illustrated that the most shallow dominant trends are NNE, NE, N-S, NNW, WNW, E-W and NW directions. While the deep structural ones are the ENE, NW, N-S, and E-W directions. This approach for edge detection used in this study is comprehensively applicable to other portions of the Egyptian Eastern Desert and other areas with alike geologic conditions around the world to give much sharper gradient over the edges of the magnetized sources which can be used for mineral and oil/gas exploration.

Keywords Samr El-Qaa · Upward continuation · Theta · HTAD · Analytic signal

Introduction

Interpretation and enhancement of magnetic data are utilized for delineating the deep and shallow geologic structures (Sharma 1997). Moreover, the edge and texture detection allowed enhancing and identifying geologic contacts like lithologic boundaries and faults (Eldosouky et al. 2017).

Mapping and detecting the edges of magnetic sources, lateral magnetic variations, is a fundamental method for mapping the geologic contacts of magnetic data. Outlining these edges is similar to constructing a geologic map with the same lithologic units, whose edges are represented as geologic contacts. For aeromagnetic grids, there are many factors that can

cause a lateral variation in magnetization other than the change in lithologies like the variation in mineral composition, metamorphism, and geologic structures, and it can reveal the alteration and deformity history of the region. Nevertheless, the edge delineation of magnetic data is a significant procedure for mapping various geologic units. Generating geologic maps from aeromagnetic data is essential in regions of overburden and large till cover. In the regions of well-exposed bedrock, the interpreters can trace connected magnetic assemblages between distinguished outcrops based on calibrated associations between lithology and anomaly shape by investigating the magnetic map. In till-covered regions, the geologic map is based particularly on interpretations of the aeromagnetic derivatives along with geophysical data; thus, accurate detection of edges is required to the map-generating process (Pilkington and Tschirhart 2017).

Dogru et al. (2016) used the edge detection methods to delineate the subsurface structures in geophysics to evaluate iron ore reserves. They concluded that the mentioned edge method was implemented to field data and gave a big agreement for the determination of the structure location.

This article is part of the Topical Collection on *New Advances and Research results on the Geology of Africa*

✉ Ahmed Mohammed Eldosouky
    ahmed.dswky@sci.svu.edu.eg

[1] Researcher at National Conservation Sector, Egyptian Environmental Affairs Agency (E.E.A.A.), Cairo, Egypt

Yan et al. (2016) used edge detection technique to interpret the potential field data for exploring the mineral, energy resources, and regional tectonics. Oliveiraa et al. (2017) proposed an algorithm to locate the edges of anomalies automatically in potential field data and to estimate the width and depth of causative sources. This algorithm found that the suggested approach presents reliable estimates for the objective parameters when compared with Euler deconvolution.

Samr El-Qaa area was studied by many authors. Said (1962) and El-Gaby (1983) illustrated the geology and tectonic setting of the study area. Bayoumi and Boctor (1970) and Abdel-Rahman and El-Etr (1980) used potential field data to detect the structural trend and the depth to the basement at Samr El-Qaa area.

The aim of the present study is to detect the edges from aeromagnetic data for delineating deep and shallow fault systems of Samr El-Qaa region using recent theta and HTAD techniques and to deduce the geologic information from the geophysical data, improve the existing edge-detection techniques, efficiency, edges continuity, reducing noise influences, and limiting the effects of variable depth to the body and source dip.

Geology of the study area

Samr El-Qaa area is located at the North Eastern Desert of Egypt, near the western side of the Gulf of Suez, to the west of Ras Gharib City (Fig. 1). The area extends between latitudes 28° 05′ 38″ N and longitudes 32° 04′ 36″ and 32° 40′ 22.76″ E, covering an area about 2400 km². Various lithologic associations ranging in age from the Precambrian to the Quaternary describe the exposed rock units in Samr El-Qaa area.

Samr El-Qaa area is dissected by several valleys, which mostly are structurally controlled and flow towards the east in the Gulf of Suez. The study area is characterized by rugged topography in its eastern part which mainly occupied by mountains of basement complex (mostly formed of granitic and volcanic rocks), while the western part is covered by sedimentary rocks, which is less complicated and mountainous than the eastern part (Hassanein and Soliman 2009).

Stern and Hedge (1985) illustrated the Eastern Desert (ED) of Egypt distinguished by three important basement zones, i.e., south (SED), north (NED), and central (CED). The CED is separated from NED by a boundary characterized by the dextral strike-slip fault (dipping NW) (Greiling et al. 1994; Stern and Hedge 1985). Stern and Hedge (1985), depending on radiogenic ages and field associations of the most types of rock units in the Eastern Desert, concluded that the NED is discriminated by the youngest rocks, while the oldest rocks are predominant in the CED and SED. The predominance of Ediacaran non-metamorphosed volcano-sedimentary

sequences (590–630 Ma), including Hammamat sediments and Dokhan volcanics (Ressetar and Monard 1983), is the main character of the NED (Breitkreuz et al. 2010).

Despite Hammamat sediments are not eternally linked to Dokhan volcanics, the northernmost appearances in the NED, including Gabal Samr El-Qaa, are represented singly by Dokhan volcanics and lack of the intercalations of Hammamat sediments. Further, plutons of the Younger Granite and dikes are dominant in the NED, whereas there is a prevailing lack of ophiolites. Older volcanics (≈ 750 Ma) (Ali et al. 2009) occur further southward in the SED and CED and are grouped into Older and Younger metavolcanics, which are assumed to be ophiolitic and island arc volcanics respectively (Stern 1981).

Various lithologic units, including many types of sedimentary, metamorphic, and igneous rocks, are the main characteristics of Samr El-Qaa area. In addition, the location of the Gulf of Suez at the eastern side of Samr El-Qaa area in the NED of Egypt gave the area more significant setting. Accordingly, the area has been studied by several authors (Bayoumi and Boctor (1970), Ammar et al. (2003), and others). The geology of Samr El-Qaa area is derived from sheet no. (NH36SW, Beni Suef, CONOCO 1987). The geologic map of the study territory (Fig. 2) describes that the area is occupied by various types of the basement and sedimentary rock units.

The geologic map of Samr El-Qaa district (Fig. 2) reveals that the eastern region of the studied territory is occupied by basement rocks. Younger granites (pink), Older granites (red), and metavolcanics are the main units of these basement rocks. Meanwhile, various types of sedimentary deposits cover the western portion of the area differing in age from the Paleozoic to Cenozoic. They consist of Araba Formation (sandstones), Samr El-Qaa Formation (shale), Wadi Qena Formation (sandstones), Galala Formation (limestone), Esna Formation (shale), Thebes Formation (limestone), Mokattam Formation, Sudr Formation, Rakhiyat Formation, Hawashiya Formation, Umm Omeiyid Formation, and Quaternary (Undifferentiated Sediments). The contact zone between the basement and sedimentary sequences is considered as an unconformity boundary (CONOCO 1987).

According to Bayoumi and Boctor (1970), the regional structure of Samr El-Qaa area is the NE-SW direction, perpendicular to the prevailing trend system of the fault systems, making horsts and grabens. Whereas Nossair (1981 and 1987) illustrated that the NE-SW, NNE-SSW, and NNW-SSE are the major structural sets and the NE-SW, NW-SE, and N-S are the predominant joint trends affecting Samr El-Qaa area.

Aeromagnetic data and methodology

In this study, reduced to the pole (RTP) data of Samr El-Qaa district was used after subtracting the International

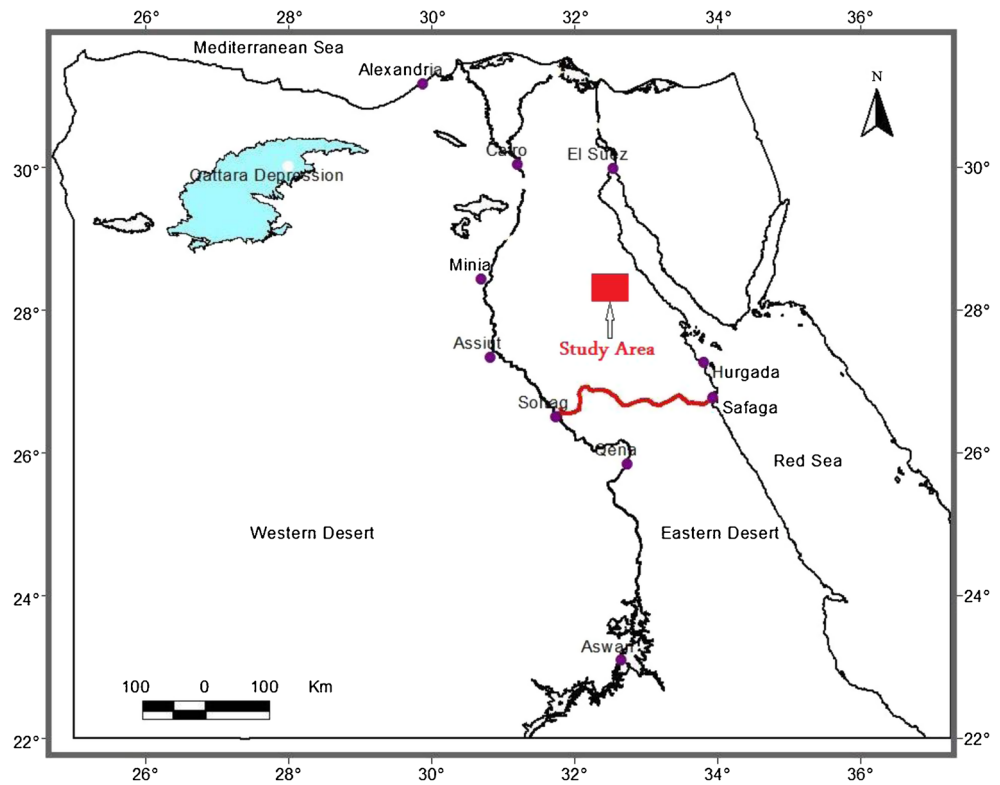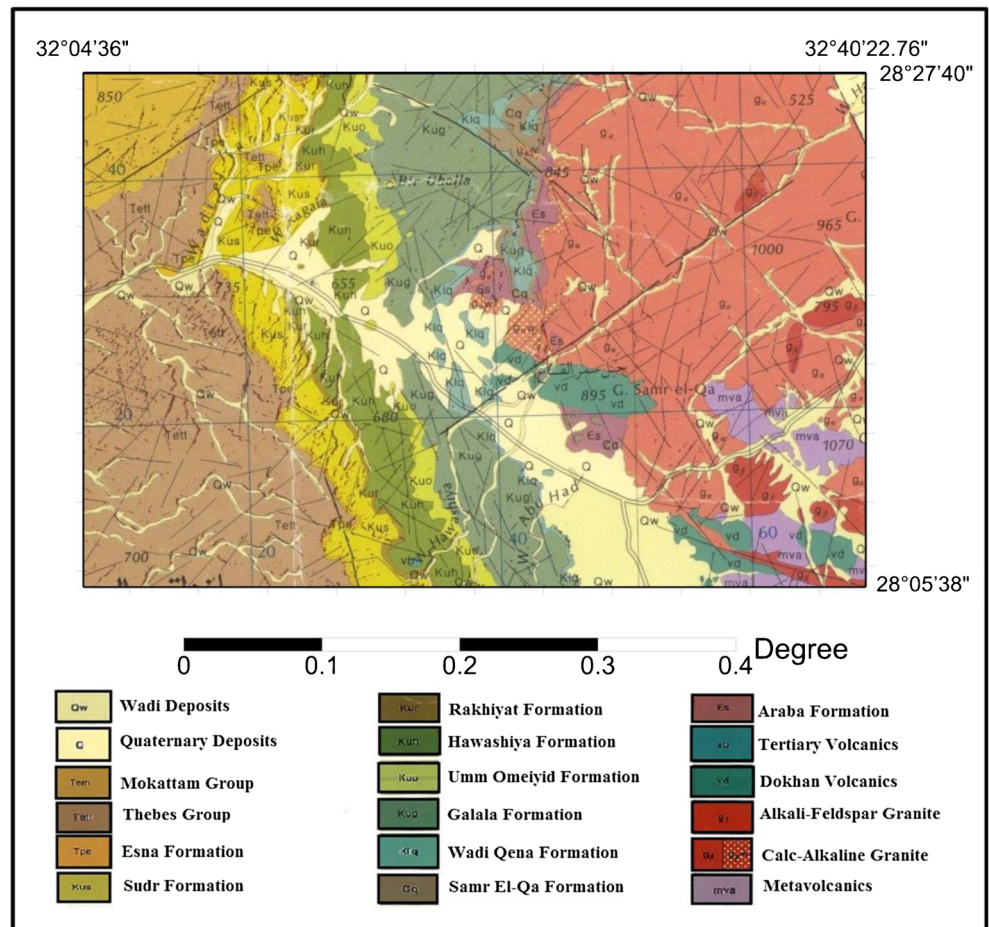**Fig. 1** Map of Egypt showing the area of Samr El-Qaa in the NED

Fig. 2 Geologic map of Samr El-Qaa area (after Conoco, 1987)

Geomagnetic Reference Field (IGRF) using the Gesoft Oasis packages (Geosoft 8.3.3 V) (Fig. 3), which is provided by the Aero Service Company (1984) for the Egyptian Mineral Resources Authority. The airborne geophysical scanning was done with a 32.8 N inclination, 1.9 E declination, and with a flight height of 120 m. Therefore, the TMI map was processed using the RTP method (Kearey and Michael 1994) after subtracting the International Geomagnetic Reference Field (IGRF) using the Gesoft Oasis packages (Geosoft 8.3.3 V).

Reduction to the pole

Pole reduction is a technique which makes the magnetic bodies appear as if observed at the pole and takes anomalies and changes their asymmetric pattern to the symmetric style (Baranov 1957). The domain of frequency is given by:

$$A'(u,v) = \frac{A(u,v)}{(\sin\theta + i\cos\theta\sin(\varphi + \alpha))^2} \tag{1}$$

where the amplitude is $A(u,v)$, α is $\tan^{-1}(v/u)$, and φ and θ are the magnetic declination and inclination.

Theta derivative

Various enhancements were practiced to appear weak anomalies of aeromagnetic maps, i.e., automatic gain control (Cooper 2009) and tilt derivative (Miller and Singh 1994). Theta derivative can produce noise in results less than the other filters when applied to downward and upward continued data (Cooper 2017).

Theta derivative was introduced by Wijns et al. (2005) for detecting the edges of magnetic anomalies. It is the ratio between the horizontal gradient magnitude (HGM) (Blakely and Simpson 1986) and the analytic signal (AS) (Roest et al. 1992) and is given by:

$$\text{Theta } (\cos\theta) = \left(\frac{\text{HGM}}{AS}\right) \tag{2}$$

Where:

$$AS(x,y) = \sqrt{\left(\frac{\partial A}{\partial x}\right)^2 + \left(\frac{\partial A}{\partial y}\right)^2 + \left(\frac{\partial A}{\partial Z}\right)^2} \tag{3}$$

$$\text{HGM}(x,y) = \sqrt{\left(\frac{\partial A}{\partial X}\right)^2 + \left(\frac{\partial A}{\partial y}\right)^2} \tag{4}$$
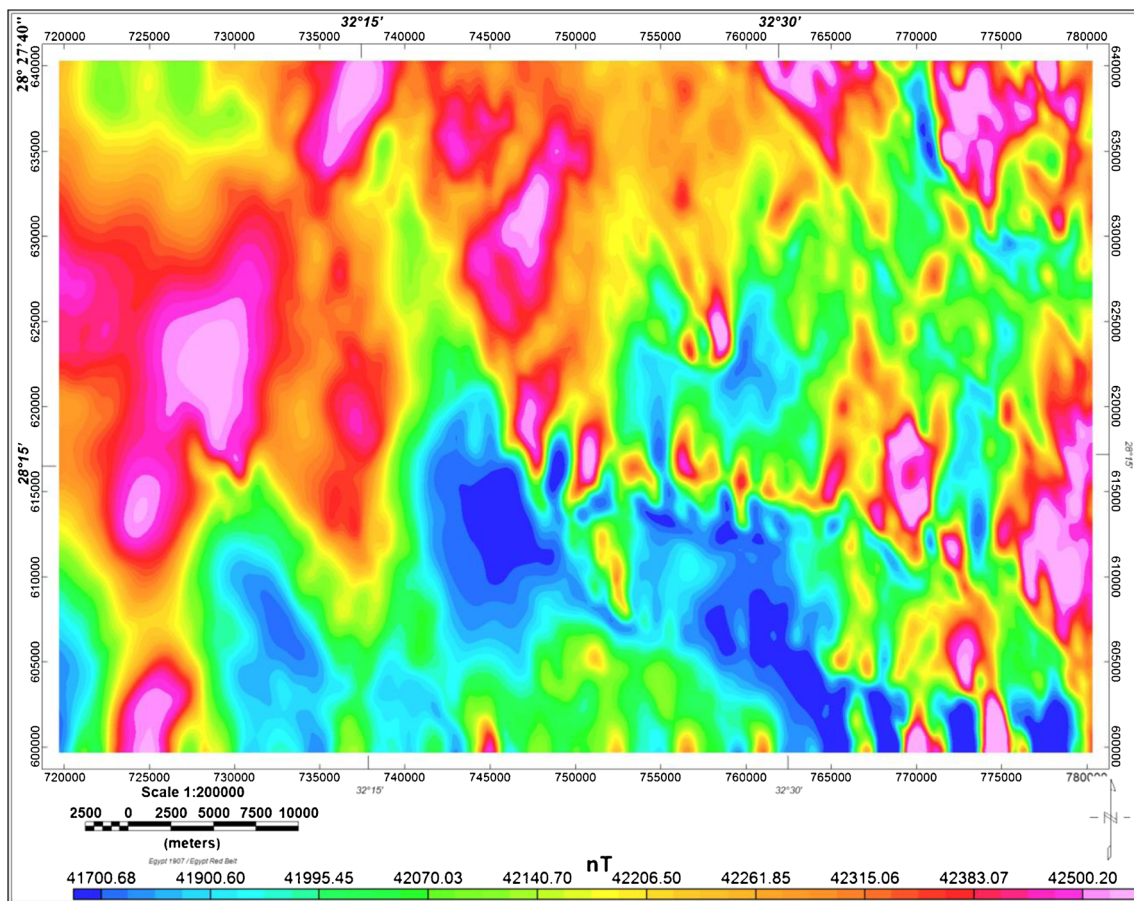

Figure 3 RTP map of Samr El-Qaa area

and $\frac{\partial A}{\partial x}$, $\frac{\partial A}{\partial y}$, $\frac{\partial A}{\partial Z}$ are the two horizontal gradients in x and y directions and the vertical gradient respectively.

Horizontal tilt angle derivative

The horizontal tilt angle derivative (HTAD) was presented by Cooper and Cowan (2006) as a method for detecting the magnetic edges. It is expressed by:

$$HTAD = \tan^{-1}\left(\frac{HGM}{\frac{\partial A}{\partial Z}}\right) \tag{5}$$

Upward continuation

Upward continuation is recognized as a distinct filter because it provides practically no side effects that may require the utilization of other enhancements to correct. It decreases the effects of higher wave number (shorter wavelength) elements associated with more local, shallower anomaly bodies; thus, it can be used as a powerful smoothing procedure for the departure of anomalies due to deeper origins. Moreover, the obtained data from upward continuation may be represented numerically and with modeling software. This is not the character for many other filter methods. The Geosoft formula to determine upward continuation is:

$$L(r) = e^{-hr} \tag{6}$$

where (h) is the distance to the continuation level and (r) is the wave number (Dobrin and Savit 1988).

Results

The methods of edge analysis (AS, HGM, theta, HTAD) were applied to RTP data.

AS and HGM of RTP data (Figs. 4 and 5) show the general fault trends affecting Samr El-Qaa territory. These two maps illustrate that the most predominant structural trends are NNE, NE, N-S, NNW, WNW, E-W, and NW directions. Moreover, the contact between the sedimentary deposits in the western part of the study region and the basement rocks in the eastern part is revealed in the HGM map of RTP (Fig. 5). However, the boundaries of faults could not be detected sharply in the results of AS and HGM of RTP data because their responses include the effects of deep structures.

The results of theta and HTAD maps (Figs. 6 and 7) provide detailed information about the geologic units and fault boundaries of Samr El-Qaa region. The fault edges and rock boundaries are well delineated in the theta and

HTAD of RTP maps. These maps (Figs. 6 and 7) clearly mapped the NE-SW fault trend direction which scattered the study area starting from the north part of Wadi Hawashiya to the northeastern part of the study region along the Alkali-feldspar granite. Moreover, the boundary between the basements to the east and the sedimentary cover to the west is sharply mapped. The edges of metavolcanics and Dokhan volcanics in the southeastern corner of the study area are clearly distinguished to be controlled along the NW, E-W, NE, NNW, and N-S directions. The good inspection of these maps showed that the eastern section (basement rocks) is more complicated in its structural pattern than the western part (sedimentary cover), where the NW, NE, NNW, E-W, N-S, and NNE directions are the main structural trends affecting the basement rocks (eastern part), while the sedimentary cover (western part) is controlled by the NW and NE directions.

The upward continuation (UC) was applied to RTP map of Samr El-Qaa area at 3 km to reveal the basement at this altitude as shown in Fig. 8. The upward continued data reveal increasing attenuation and broadening of the high wave number anomalies with increasing altitude above the investigated area.

The same methods of edge analysis (AS, HGM, theta, and HTAD) were applied to the UC data. The response of AS and HGM of UC (3 km) (Figs. 9 and 10) from deep sources does not provide the assumed sharp slope over the magnetic edges. They give a general picture of the subsurface faults.

Otherwise, the theta and HTAD maps (Figs. 11 and 12) of UC (3 km) give more information about the subsurface geologic rock units of the area. Theta map (Fig. 11) delineates deep fault edges well. The N-S, ENE, NW, NNE, and NE are the main deep fault patterns at Samr El-Qaa. HTAD map (Fig. 12) of UC (3 km) sharply outlined and mapped the edges and boundaries of deep geologic units. The golden-yellow line in Fig. 12 represents the magnetic edges of deep units and structures.

Discussion

Figure 13a and b represents the interpreted structural maps derived from shallow and deep theta and HTAD maps of Samr El-Qaa territory to illustrate the prevailing tectonic pattern in the study area.

The delineated structural elements in the shallow structural map (Fig. 13a) are statistically investigated by considering the azimuth and the number of aeromagnetic lineaments in each 10° and are displayed in the form of the rose diagram as shown in Fig. 14a. The shallow rose diagram (Fig. 14a) shows that the most dominant trends are arranged in the NNE, ENE, NNW, N-S, E-W, and WNW directions.
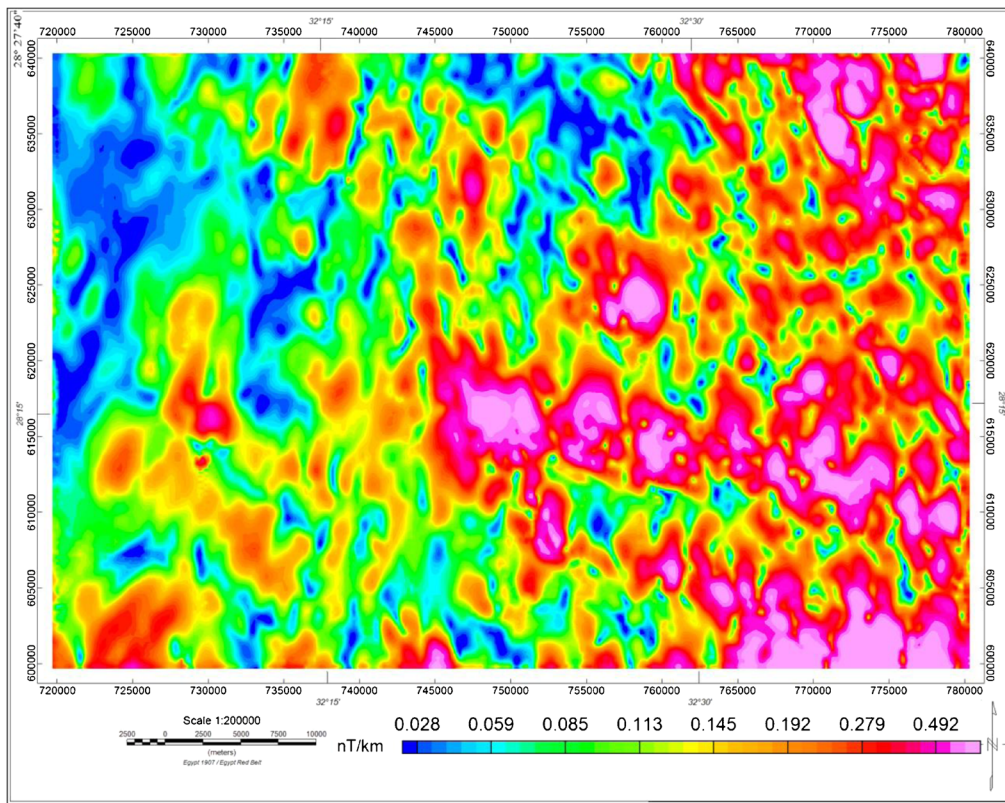
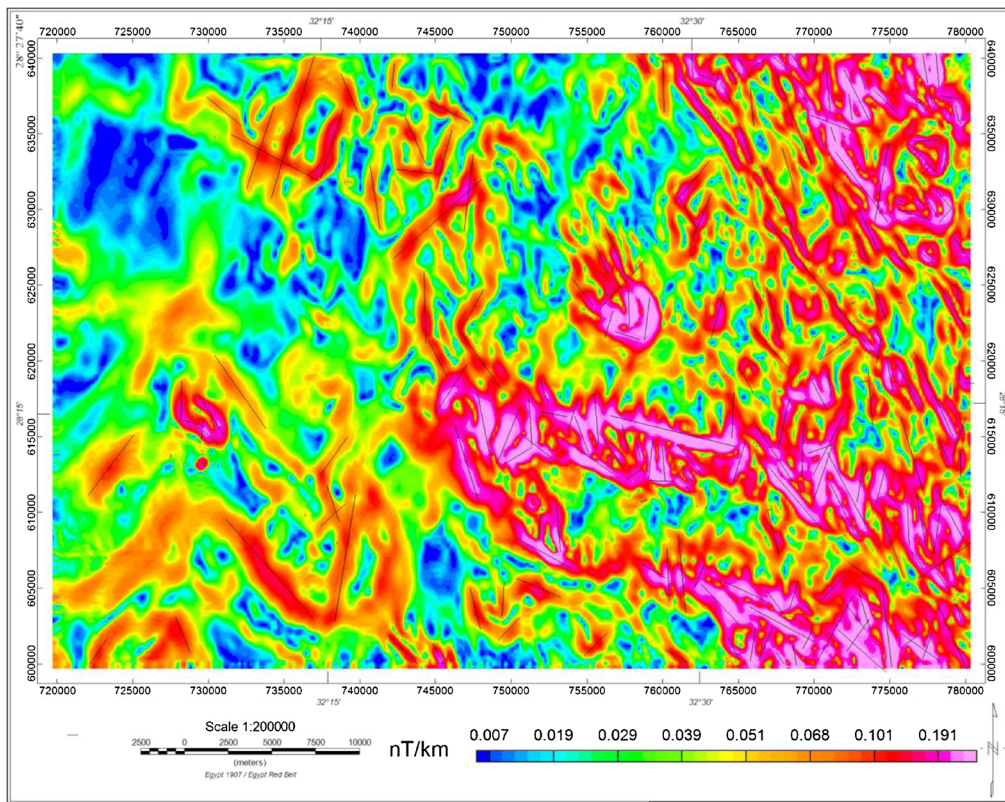**Fig. 4** AS map of RTP data of Samr El-Qaa area
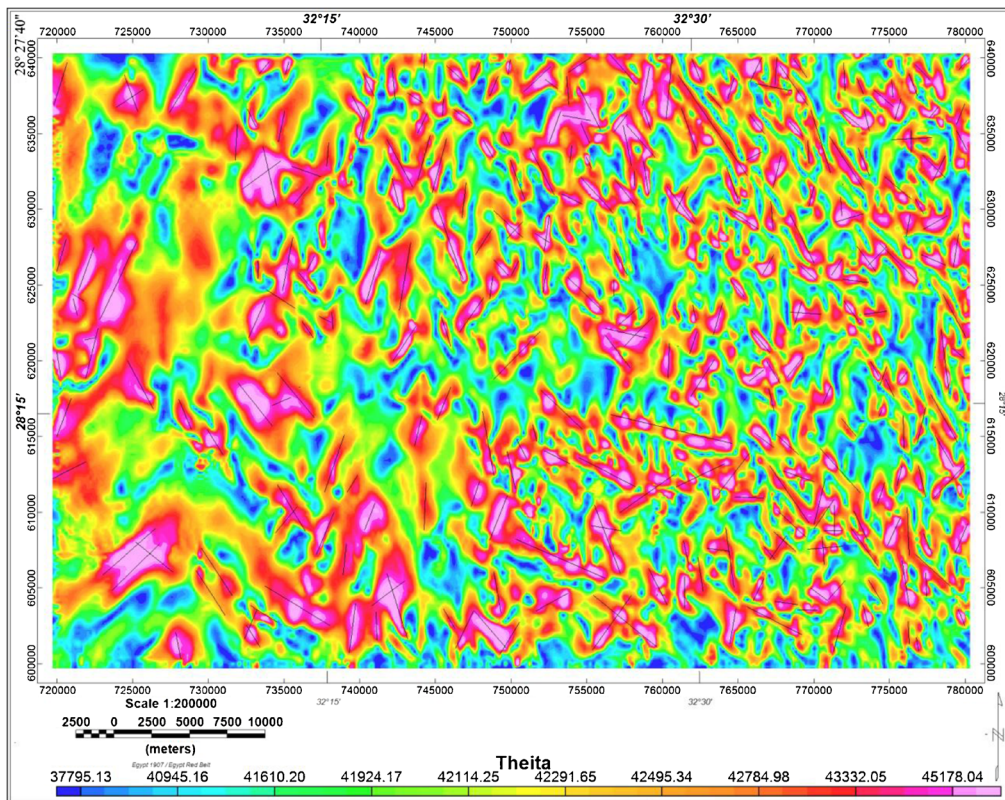

Fig. 5 HGM map of RTP data of Samr El-Qaa area

Fig. 6 Theta map of RTP data of Samr El-Qaa area
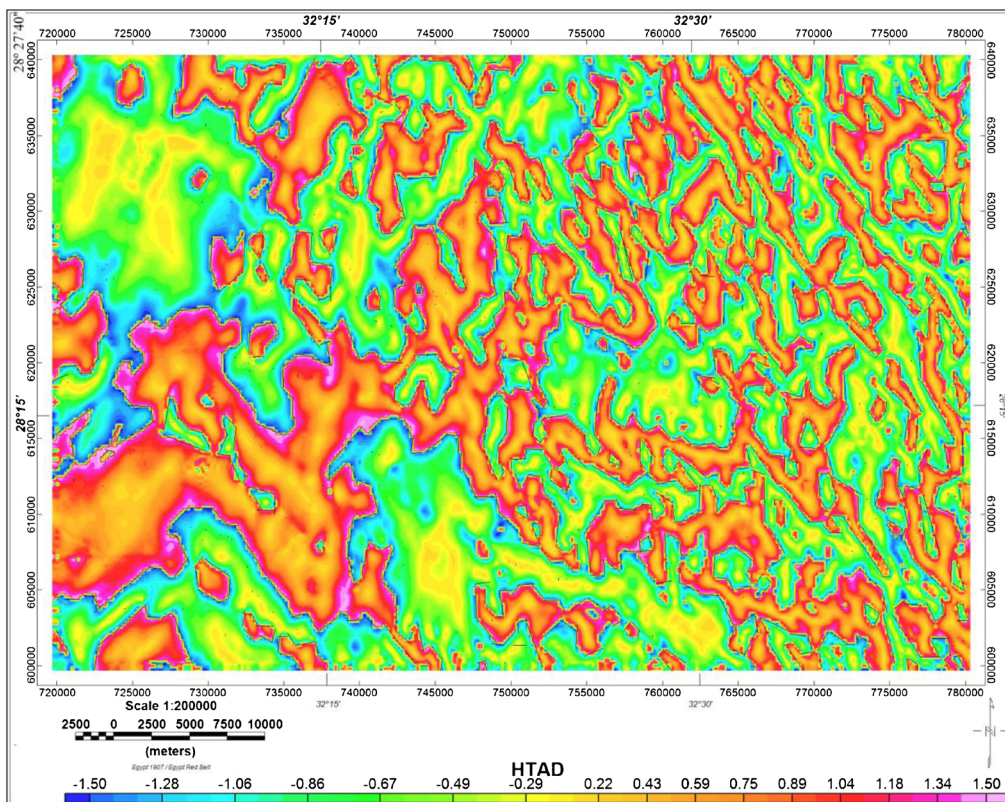

Fig. 7 HTAD map of RTP data of Samr El-Qaa area
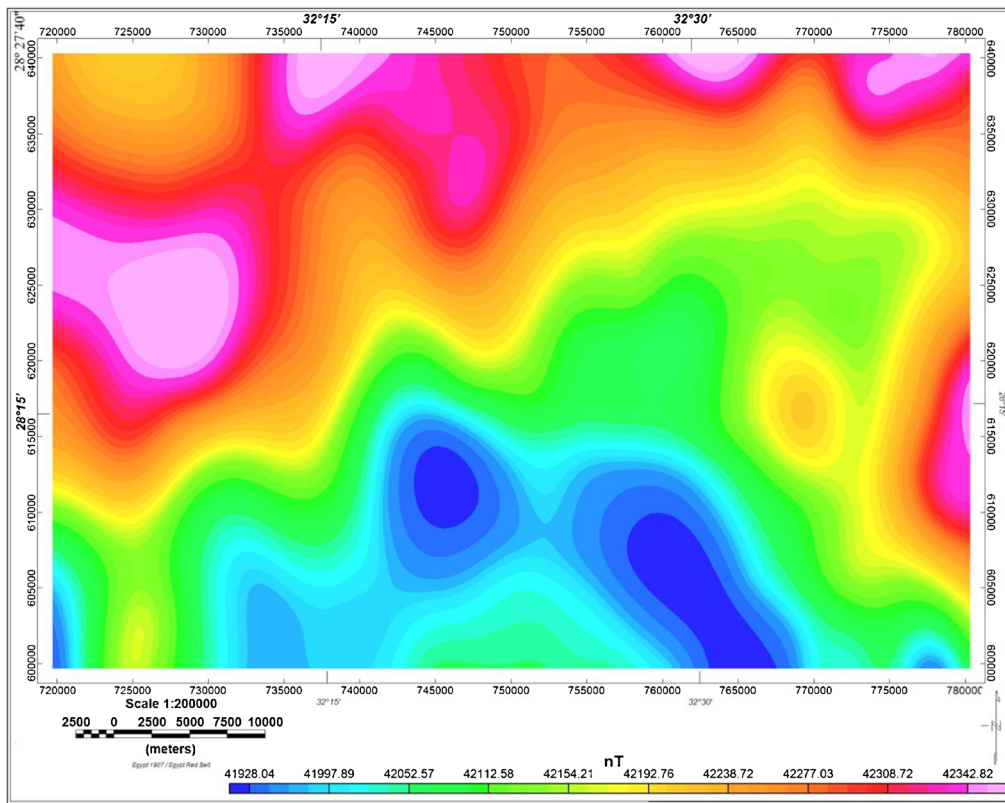
Fig. 8 UC map of Samr El-Qaa area (3 km level)
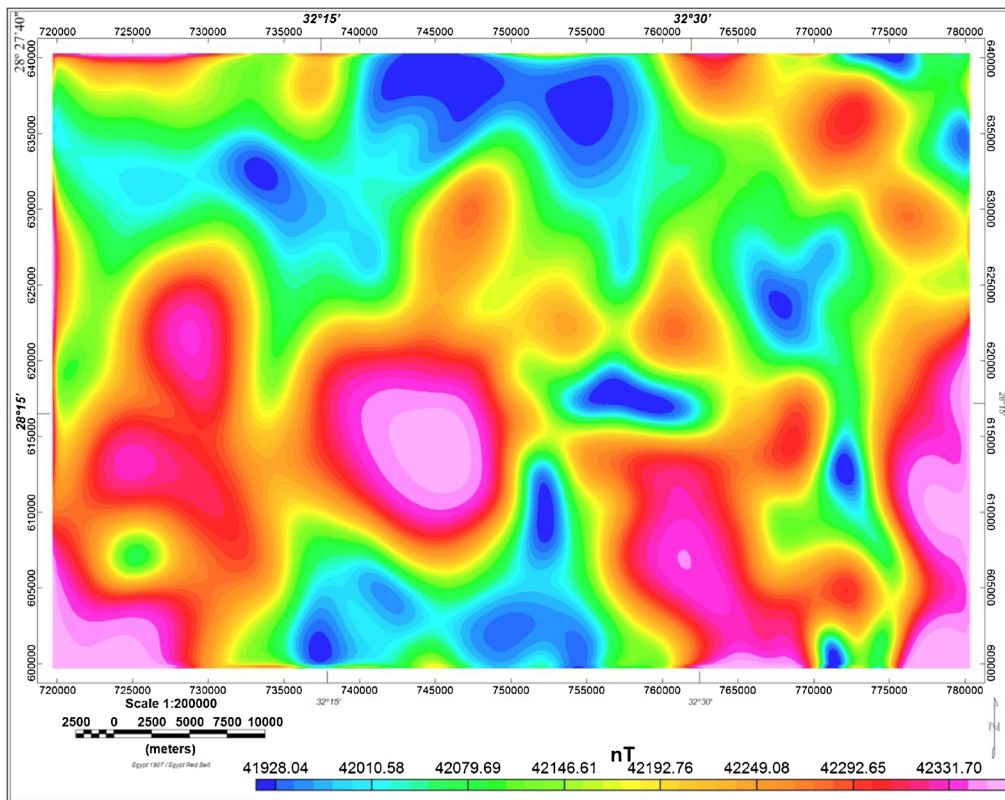

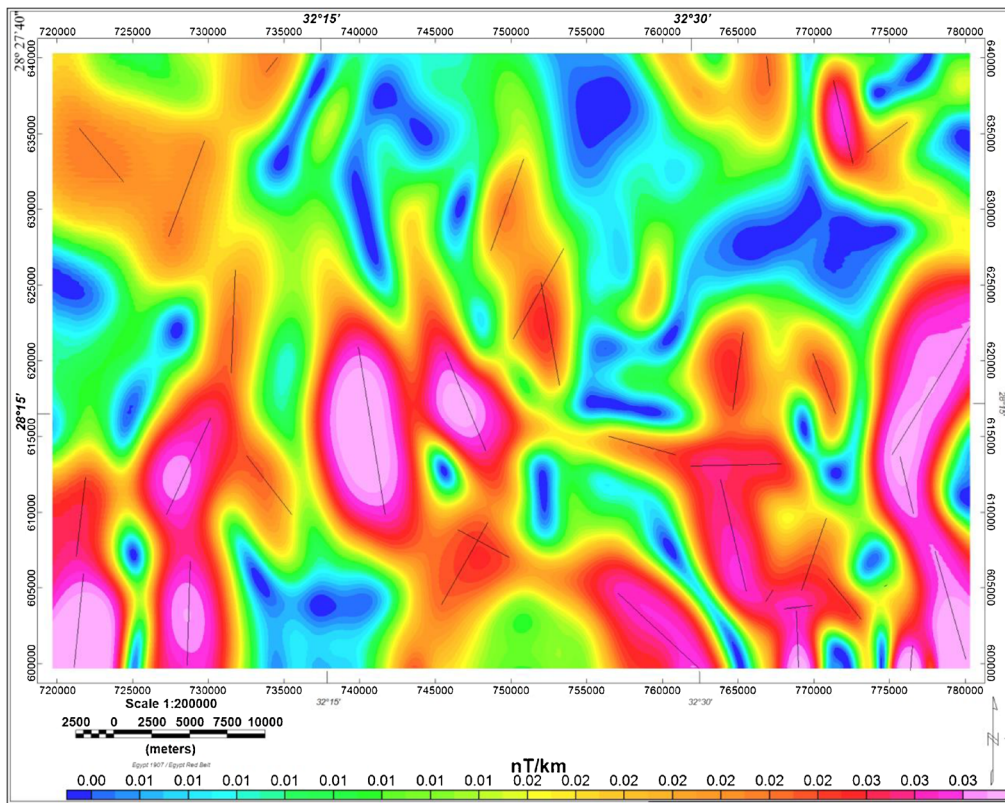**Fig. 9** AS map of UC (3 km) of Samr El-Qaa area

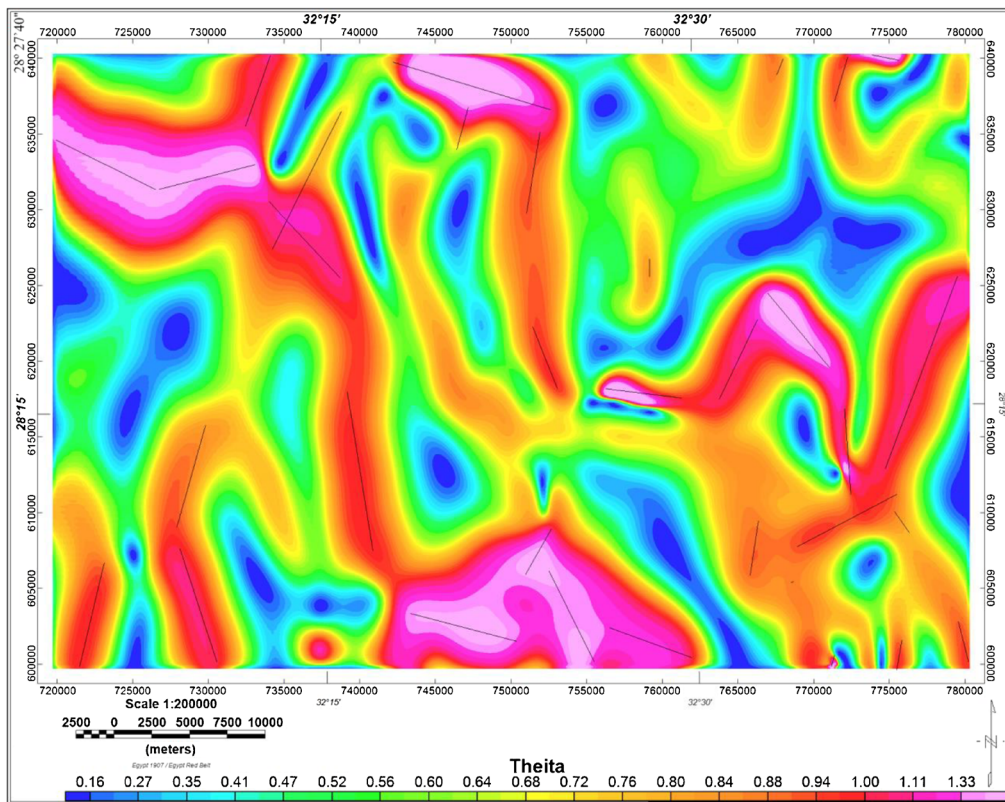**Fig. 10** HGM map of UC (3 km) of Samr El-Qaa area

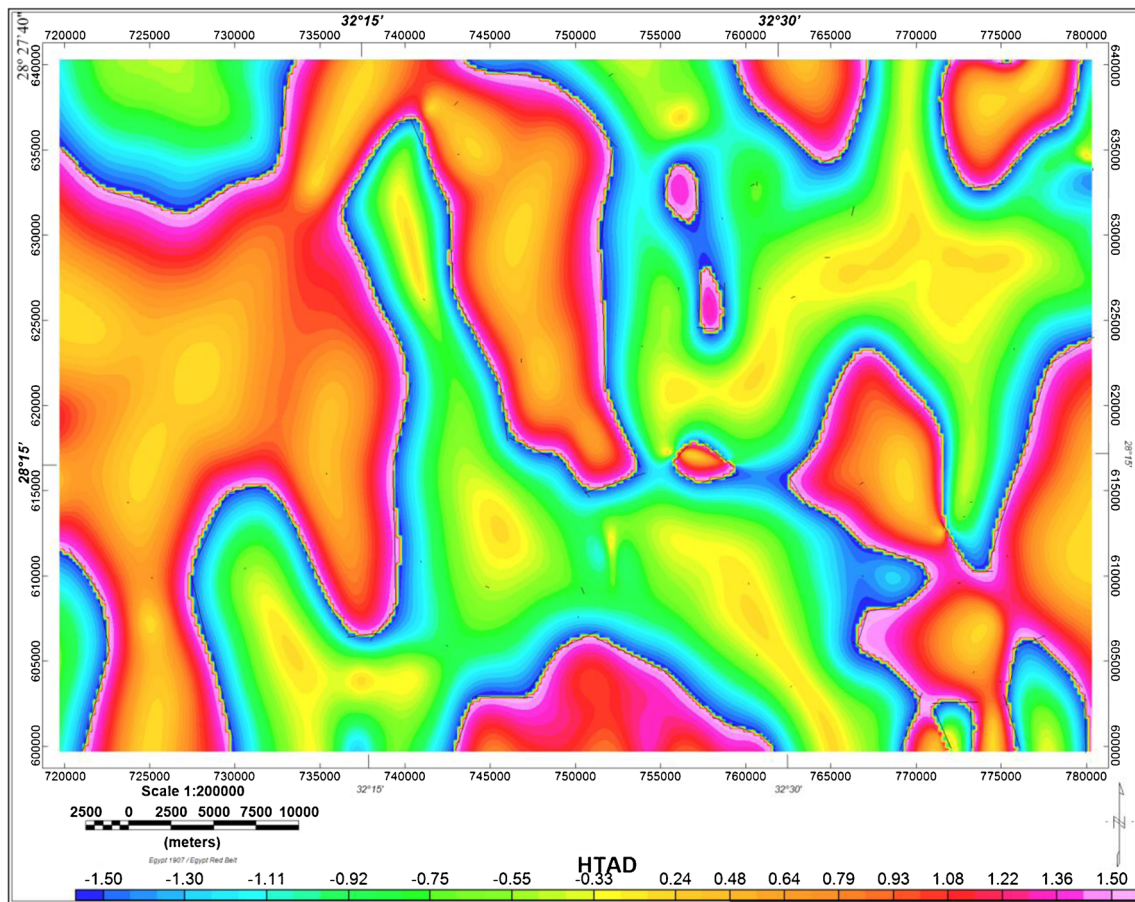**Fig. 11** Theta map of UC (3 km) of Samr El-Qaa area

Fig. 12 HTAD map of UC (3 km) of Samr El-Qaa area

The deep structural map (Fig. 13b) and the deep rose diagram (Fig. 14b) indicate that the ENE, N-S, E-W, NNW, and NW directions are the main subsurface structural trends controlling Samr El-Qaa area. Moreover, NNE direction was the dominant trend in the geologic and shallow structural maps and appeared as a minor trend in the deep altitudes indicating that it is the youngest structural trends controlling Samr El-Qaa district.

According to Meshref and El-Sheikh (1973), the NNE (Aqaba) trend is the prevailing tectonic trend and Sinai and the Gulf of Aqaba. It is probably a common shallow cross-trend in the Red Sea and Suez Gulf fault block mosaic. While the N-S (East-African) trend was considered as one of the oldest fractures in the Egyptian Eastern Desert (EED) (Tealeb 1979), moreover, the E-W (Tethyan) trend was considered as the oldest fault pattern in Egypt and the oldest tectonic fault affecting the basement of Egyptian (El-Shazly 1966). The N-S and E-W trends were the predominant tectonic faults affecting the study region as shown in the shallow and deep structural maps (Fig. 14a, b).

Theta and HTAD edge detector methods were applied for enhancing magnetic anomalies for sharp detection of magnetic features and source edges of Samr El-Qaa territory that equalize signals from ear surface and deep sources. The effectiveness of the approach is estimated by correlating it with other edge detection techniques that have been earlier described in the literature and that make application of derivatives. The results confirm that theta and HTAD are less sensitive to the depth variation of the sources and that they map the location of the causative body edges in an extra accurate way when compared with previous AS and HGM methods, also for anomalies due to multiplied interfering origins. These results display that the theta and HTAD methods are useful tools for interpreting the magnetic data qualitatively.

Calculated edge locations estimated from these methods appear sufficiently accurate, less sensitive to noise, and continuous, and detailed outcomes to afford a stable basis on which the mapping operations were based and achieved successfully.
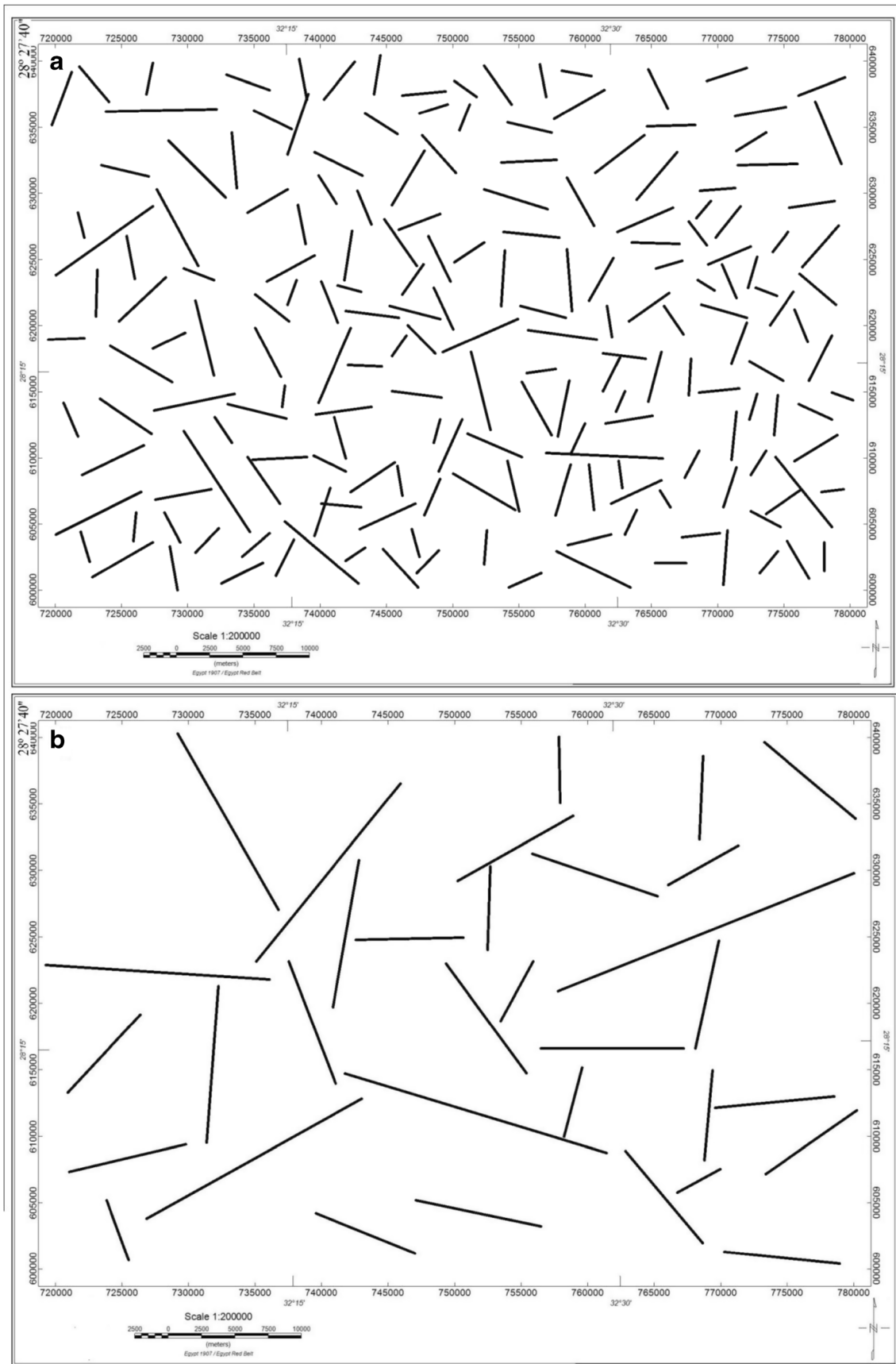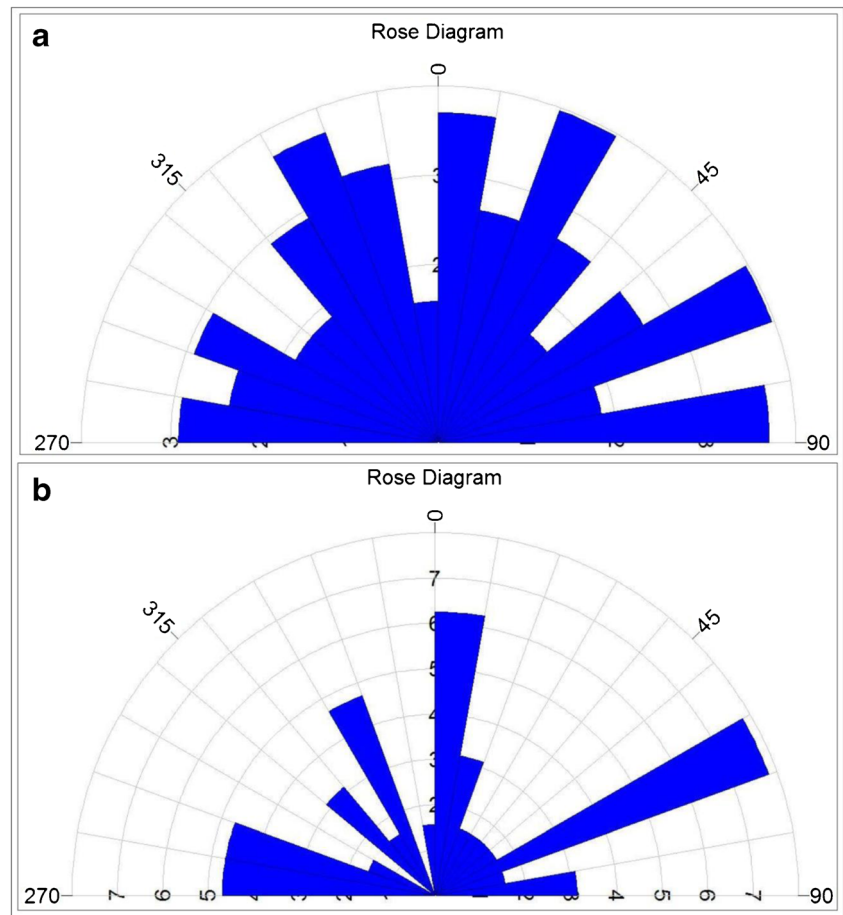
Fig. 13 Shallow structural map (**a**) and deep structural map (**b**) of Samr El-Qaa area

Fig. 14 Shallow rose diagram (**a**)
and deep rose diagram (**b**) of
Samr El-Qaa area

Conclusions

AS, HGM, theta, and HTAD methods were applied to RTP
and upward continued (UC) (3 km) data of Samr El-Qaa area
to define the edges of surface and deep geologic units and fault
boundaries. AS and HGM maps of RTP data illustrated that
the most predominant shallow structural trends are arranged in
the NNE, ENE, NNW, N-S, E-W, and WNW directions, but
the response of AS and HGM of UC (3 km) from the deep
sources does not provide the assumed sharp slope over the
magnetic edges.

The theta and HTAD maps of RTP and UC (3 km)
data provide more information about the shallow and
subsurface geologic rock units. Theta map successfully
delineated fault edges, while HTAD map sharply outlined
and mapped the edges and boundaries of geologic rock
units.

As a general conclusion, it can be concluded that the AS,
HGM, theta, and HTAD techniques were successfully applied
for outlining the edges of aeromagnetic data at Samr El-Qaa
territory.

The present study illustrated that the estimated edge posi-
tions calculated from the theta and HTAD techniques are

sufficiently reliable and continue to give a solid basis on
which the mapping operations were based and accomplished
successfully. The theta and HTAD approach used in this study
are broadly suitable to other parts of the Egyptian Eastern
Desert and other districts with related geological conditions
in Africa and the world which can be used for mineral and oil/
gas exploration.

References

Abdel-Rahman MA, El-Etr HA (1980) The orientational characteristics
of the structural grain of the Eastern Desert of Egypt. In: El-Etr HA,
Embabi NS, Youssef MSM (eds) Geologic-Geomorphic Studies in
the Egyptian Deserts. Ain Shams Uni, Cairo, Egypt (Abstract), 5 p

Aero-Service (1984) Final operational report of airborne magnetic/ radi-
ation survey in the Eastern Desert, Egypt, conducted for the
Egyptian General Petroleum Corporation, Aero- Service Division,
Houston. In: Western geophysical co. Taxas, USA

Ali KA, Stem RJ, Manton WI, Kimura JL, Khamees HA (2009)
Geochemistry, Nd isotopes and U–Pb SHRIMP dating of
Neoproterozoic volcanic rocks from the Central Eastern Desert of
Egypt: new insights into the ≈750 Ma crust-forming event.
Precambrian Res 171:1–22

Ammar AA, Abdel-Rahman MA, Hassanein HIE, Soliman KS (2003) Radiometric lithologic interpretation of aerial radiospectrometric false colour image maps, Eastern Desert, Egypt. Arab Gulf J Sci Res 21(1):28–47

Baranov V (1957) A new method for interpretation of aeromagnetic maps: pseudo-gravimetric anomalies. Geophysics 22:359–383

Bayoumi AI, Boctor JG (1970) Geological significance of gravity and magnetic anomalies in Rahmi area, Gulf of Suez district, U.A.R. 7th Arab Pet. Con., Secret. Gen. Leag. Arab State, Kuwait, Mar. 1970, 2 (36): B-2, 28 p

Blakely RJ, Simpson RW (1986) Approximating edges of source bodies from magnetic or gravity anomalies. Geophysics 51(7):1494–1498

Breitkreuz C, Eliwa H, Khalaf I, El Gameel K, Bühler B, Sergeev S, Larionov A, Murata M (2010) Neoproterozoic SHRIMP U–Pb zircon ages of silica-rich Dokhan volcanics in the North Eastern Desert, Egypt. Precambrian Res 182:163–174

Conoco Coral (1987) Geological map of Egypt, scale 1: 500,000, - NH36SW- Beni Suef, Egypt. The Egyptian General Petroleum Corporation, Cairo (EGPC), Egypt

Cooper GRJ (2009) Balancing images of potential field data. Geophysics 74(3):L17–L20

Cooper GRJ (2017) A tale of three filters; the tilt angle, the theta map, and sunshading. Extended Abstracts - 15th SAGA Biennial Conference & Exhibition

Cooper GRJ, Cowan DR (2006) Enhancing potential field data using filters based on the local phase. Comput Geosci 32(10):1585–1591

Dobrin MB, Savit CH (1988) Introduction to geophysical prospecting 4th Edn. McGraw Hill Book Co., New York

Dogru F, Oya Pamukcu O, Cagatay Pamukcu C (2016) Determination of mine location by using edge detection methods: a case study of Sivas-Divrigi. Earth Sci 5(4):56–61. https://doi.org/10.11648/j.earth.20160504.12

Eldosouky AM, Abdelkareem M, Elkhateeb SO (2017) Integration of remote sensing and aeromagnetic data for mapping structural features and hydrothermal alteration zones in Wadi Allaqi area, South Eastern Desert of Egypt. J Afr Earth Sci 130(2017):28–37

El-Gaby S (1983) Architecture of the Egyptian basement complex, Proceed. 5th Intern. Conf. Basement Tectonics, Cairo, Egypt.

El-Shazly EM (1966) Structural development of Egypt, U.A.R.. Abstract of the 4th Annual Meeting, Geol. Society of Egypt, Cairo, Egypt, pp. 31–38

Greiling RO, Abdeen MM, Dardir AA, El Akhal H, El Ramly MF, Kamal El Din GM, Osman AF, Rashwan AA, Rice AHN, Sadek MF (1994) A structural synthesis of the Proterozoic Arabian-Nubian Shield in Egypt. Geol Rundsch 83:484–501

Hassanein HIE, Soliman KS (2009) Aeromagnetic data interpretation of Wadi Hawashiya area for identifying surface and subsurface structures, North Eastern Desert, Egypt. JKAU: Earth Sci 20(1):117–139

Meshref WM, El-Sheikh MM (1973) Magnetic-tectonic trend analysis in northern Egypt. J Geol 17(2):179–184

Kearey P, Michael B (1994) An introduction to geophysical exploration. vol 8. Nos. 2,3 & 4. Blackwell Sciences, pp 183–190

Miller HG, Singh V (1994) Potential field tilt – a new concept for location of potential field sources. J Appl Geophys 32:213–217

Nossair LM (1981) Relation of radioactivity to fracture system in some basement rocks, North Eastern Desert, Egypt, M. Sc Thesis (Unpub.), Fac. Sci., Al-Azher University, Egypt.

Nossair LM (1987) Structural and radiometric studies on Gabal Gharib area, North Eastern Desert, Egypt, Ph.D. Thesis (Unpub.), Fac. Sci., Alexandria University, Egypt.

Oliveiraa SP, Ferreirab FJF, de Souzac J (2017) EdgeDetectPFI: an algorithm for automatic edge detection in potential field anomaly images – application to dike-like magnetic structures. Comput Geosci 103:80–91

Pilkington M, Tschirhart V (2017) Practical considerations in the use of edge detectors for geologic mapping using magnetic data. GEOPHYSICS 82(3):J1–J8 8 FIGS

Ressetar R, Monard JR (1983) Chemical composition and tectonic setting of the Dokhan volcanic formation, Eastern Desert, Egypt. J Afr Earth Sci 1:103–112

Roest WR, Verhoef V, Pilkington M (1992) Magnetic interpretation using the 3-D analytic signal. Geophysics 57:116–125

Said R (1962) The geology of Egypt. Elsevier Publ. Co., Amsterdam-New York 337 p

Sharma PV (1997) Environmental and engineering geophysics. Cambridge University Press, Cambridge

Stern RJ (1981) Petrogenesis and tectonic setting of late Precambrian enzymatic volcanic rocks, Central Eastern Desert of Egypt. Precambrian Res 16:195–230

Stern RJ, Hedge CE (1985) Geochronologic and isotopic constraints on late Pre-cambrian crustal evolution in the Eastern Desert of Egypt. Am J Sci 285:97–127

Tealeb A (1979) Predominant tectonic trends in North Egypt. Academy of Scientific Research & Technology, Helwan Institute of Astronomy and Geophysics, Bulletin No 189

Wijns C, Perez C, Kowalczyk P (2005) Theta map: edge detection in magnetic data. Geophysics 70(4):39–43

Yan TJ, Wu YG, Yuan Y, Chen L–N (2016) Edge detection of potential field data using an enhanced analytic signal tilt angle. Chin J Geophys (in Chinese) 59(7):2694–2702. https://doi.org/10.6038/cjg201607.